



## Reconfigurable Circularly Polarized Antenna for WLAN and WiMAX

<sup>1</sup>Mohamed Bikrat, <sup>2</sup>Seddik Bri

<sup>1,2</sup>Electrical Engineering Department, High School of Technology: ESTM Moulay Ismail University, B. P 3103, Meknes, Morocco

<sup>1</sup>bikratmed@gmail.com, <sup>2</sup>briseddik@gmail.com

### ABSTRACT

A simple design for a bi-band circularly polarized (CP) antenna with the capability of switching its polarization between dual-sense CPs is presented in this article, by using a monopole loop antenna as a primary radiator as a proposed antenna. An additional CP band is achieved by controlling the ON/OFF states of two PIN diodes; moreover, the reconfigurability of the polarization between right-hand CP (RHCP) and left-hand CP (LHCP) at three different frequencies 2.8, 3.4 and 4 GHz is realized. For validation, a retractable patch antenna design is offered on the basis of a distinctive situation analysis. The antenna offers a low reconfigurable band and a fixed band at higher frequencies. It also presents a reconfigurable low band and a fixed band at higher frequencies where the antenna has a simulated 3 dB ARBW of 52.8% [1.9-2.5] GHz, while the axial ratio bandwidths for both the RHCP and LHCP states were 5.1% [1.9-2] GHz, 8% [2.4-2.6] GHz, and 52.8% [1.9-2.5] GHz. Located in a reflection bandwidth of -10 dB of 3% [1.62-1.67] GHz, 8% [2.4-2.6] GHz for RHCP and 3% [1.62-1.67] GHz, 8% [2.44-2.64] GHz for LHCP. The proposed antenna is suitable for wireless applications such as WLAN (2.5 GHz) and part of the medium band of WiMAX..

**Key words:** Reconfigurable antenna, broadband antenna, circular polarization, bi-band.

### 1. INTRODUCTION

In many telecommunication applications, particularly for the radio-relay, systems must radiate in circular polarization antennas with outstanding features and exhibit many advantages over linearly polarized (LP) antennas, including the ability to mitigate polarization mismatch and establish stable communication between the transmitter and receiver sides.

In recent years circularly polarized (CP) antennas with the capability of switching polarization between right-hand CP (RHCP) and left-hand CP (LHCP) states have increasingly been used in wireless communication systems [1-2].

Therefore, this article presents a two-band antenna suitable for WLAN applications. The work proposed proposes a

similar simulation approach, but only in the 5 GHz band. However, the proposed antenna operates at 3.4 GHz band, which will be a reconfigurable band. Technically our work has been proposed to transform the polarization from linear mode to circular mode. However, these modifications yield narrower 3 dB ARBW than impedance bandwidth (IBW). Such as, improving the 3 dB ARBW technique is necessary. Many methods have been investigated for this purpose. On the one hand, these modifications improve the impedance bandwidth, axial ratio bandwidth, and gain.

To achieve these needs, the first solution is to design antennas with strip-band properties and reconfigurable polarization [3-10]. Array antennas adopted a Wilkinson power divider [3] and a phase shifter with a power divider [4], for broadband coaxial bandwidth (ARBW). These antennas, however, requires complex webs to feed. Other antennas were of simple feeding Explore in [3-8]. It can consist of an electrode [5] or a magnetic electrode and a mixture of dipole [6-7]. This is a wide-open end formation and has a tapered composition, which elicits a multi-method resonance to achieve broad CP. Instead of using the PIN diode electrical switching technique [1-5], other techniques have been suggested in [8-9]. The water spiral structure is used to perform broadband CP in [8]. The water spiral structure was used to perform broadband CP. By controlling the water flow between the two channels, the antenna polarization is adjusted. Besides, MEMS switches are used on an E-shaped radiator to achieve CP reshaping [9]. The two E-shaped gaps are used to create various electrical paths, which spark a multi-mode echo to achieve a wide range. Compared to the PIN diode, the hydro-helical structure and MEMS switches seem to cause difficulty in the manufacturing process and / or increase the cost. In addition, one of the prominent barriers to broadband antennas is known to be interference with other radio equipment communication systems.

To address this issue, the multi-band reconfigurable antennas have been investigated. In addition, unipolar structures or openings are commonly used [10-12]. Arrow keys are set symmetrically and the antenna can be switched between circular and linear polarization. The method of the load switches on the feed structure in [13-15] is used to change the antenna operating states. A feed network is used to reconstruct LP / LHCP / RHCP in [14] and impedance

bandwidth is obtained for both circular and linear polarization. In [15], the antenna can provide both LP / CP by adjusting the bias states of the variable diodes on the feed network.

Our objective in this article is the development of a new proposed antenna reconfigurable in order to achieve a multi-band CP antenna with radiation characteristics the bidirectional polarization. This will allows us to find the best antenna performance concerning the gain and bandwidth. The proposed design is able to demonstrate two-sense CP realization at three different frequencies, by switching the state of two PIN diodes.

The article is divided into four sections. We will start with the design proposed antenna geometry. The second section describes the evolution of the proposed antenna design in order to ameliorate its performance. In the third section, we will examine and discuss the influence of the main parameters on the antenna performance. Finally, the last section presents our proposed PIN-Diode and Switching of the CP-Sense and its effects.

## 2. ANTENNA DESIGN

The geometry of the proposed antenna is illustrated in Fig 1. The proposed bi-band reconfigurable CP antenna is formed of a square-ring radiator, a parasitic loop and PIN diodes; the antenna consists of a rectangular patch with

length  $L$  and width  $W$ , where entire dimensions of the ground plane are  $L_s \times W_s$ . The substrate used is Rogers RO3003, which is a loss substrate with a dielectric constant of  $\epsilon_r = 3$  and loss tangent  $\tan \delta = 0.001$ . The evolution process and the simulated  $S_{11}$  of the proposed antenna for each configuration are shown in Fig 2 and 3, respectively. The antenna was simulated using the commercial ANSOFT High-Frequency Structure Simulator (HFSS). A detailed description of each configuration listed as follows.

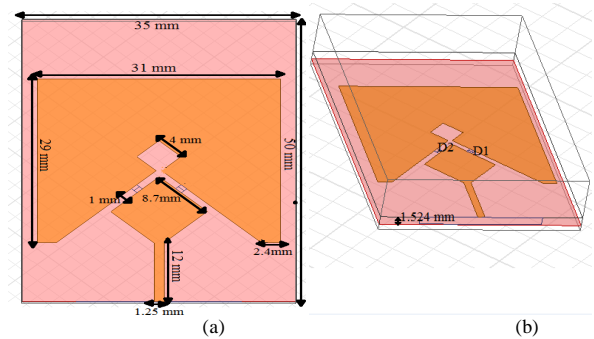


**Figure 1** : The basic geometry of the reference antenna (a): front view and (b): side view. Separation between the two plates is 1.524 mm

## 3. Evolutionary procedure for the proposed antenna

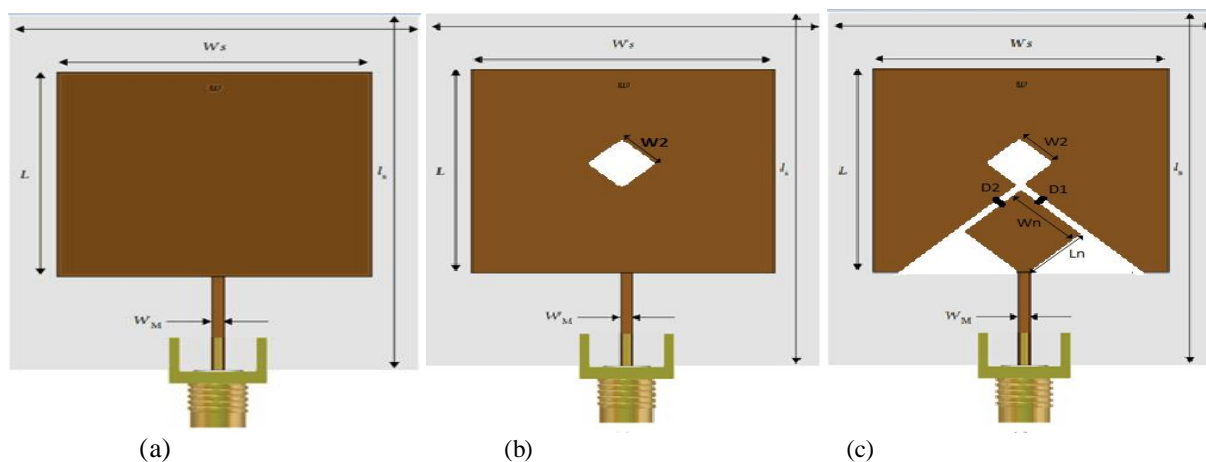


**Figure 2** : Evolutional procedure for the proposed antenna: (a) Configuration 1; (b) Configuration 2; (c) Configuration 3

Figure 2 shows the Evolutional procedure for the proposed antenna .by varying the dimensions of the antenna. After many optimizations by HFSS as shown in Figure 3, the dimensions are shown in Figure 1. A patch antenna is implemented by etching off different shapes in the patch, which disturbs the shield current distribution depending on the configuration of the defect. This disturbance will influence the components of a transmission line, for example, line capacitance and inductance. It can also manage

the electromagnetic wave propagating into the substrate layer and excitation. Energy is focused around the patch antenna, In other words, any defect etched off in the metallic patch of the microstrip leads to increasing effective inductance and capacitance.

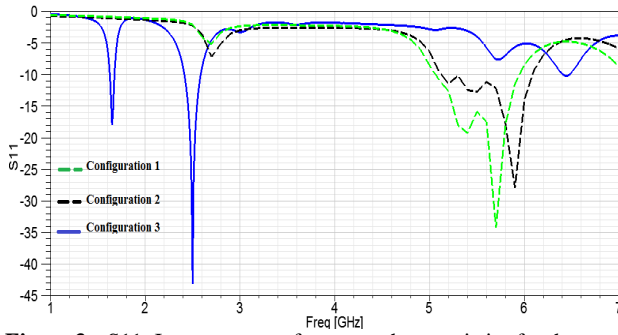


**Figure 3 :** S11: Improvement of antenna characteristics for three design configurations.

**Configuration 1:** In this configuration, Reconfigurable Antenna Simulation and Methods. As can be observed in Figure 2, is fed by a 50-Ω transmission, with linear polarization properties. We see that the reflection coefficient S11 is less than -35 dB over the entire band at the resonant frequency of 5.7 GHz. The bandwidth of the reflection coefficient at -10 dB is approximately 0.92 GHz. On the other hand, we note that there is only one PIC of the resonance frequencies present in the band the frequencies from 5.04 GHz to 5.96GHz as shown in Figure 3.

**Configuration 2:** The closed-loop square radiator is fed with a closed-loop by a 50-Ω transmission line. The closed-loop radiator generates an unloaded position and the square ring is rotated 45° around the z-axis and fed to a corner. As shown in Figure 2 with linear polarization properties, we can see that the reflection coefficient S11 is less than -30 dB over the entire band at the resonant frequency of 5.9 GHz. The bandwidth of the reflection coefficient at -10 dB is approximately 0.98 GHz. but a resonance frequency PIC has an ultra-wideband from 5.12GHz to 6.1GHz.as shown in Figure 3. For a conventional circular antenna, resonance is estimated using the following equation [16]. Figure 2 shows the Evolutional procedure for the proposed antenna .by varying the dimensions of the antenna. After many optimizations by HFSS as shown in Figure 3, the dimensions are shown in Figure 1. A patch antenna is implemented by etching off different shapes in the patch, which disturbs the shield current distribution depending on the configuration of the defect. This disturbance will influence the components of a transmission line, for example, line capacitance and inductance. It can also manage the electromagnetic wave propagating into the substrate layer and excitation. Energy is focused around the patch antenna, In other words, any defect etched off in the metallic patch of the microstrip leads to increasing effective inductance and capacitance

**Configuration 3:** In this configuration, the square ring is rotated 45° around the z-axis [17–20] by using the Bandwidth and gain improvement of a circularly polarized dual-rhombic loop antenna in [17] and Broadband circularly polarized crossed dipole with parasitic loop resonators and its arrays in [18].Etching off two rectangles and two triangles in the patch, and fed in one corner. The PINs, D1 and D2 using techniques to Dual-band reconfigurable circularly

polarized monopole antenna in [21] are inserted into the radiant arm of the square ring which disturbs the shield current distribution depending on the configuration of the defect. This disturbance will influence the components of a transmission which disturbs the shield current distribution depending on the configuration of the defect. This disturbance will influence the components of a transmission line [22–24]. To further improve the IBW, Configuration 3 is performed. A technique of using a notch antenna plane to fine-detune the antenna’s input impedance, which has been thoroughly investigated in [25], is applied. The notch antenna only affects IBW at a high-frequency region, which ARBW of reflection bandwidth of -10 dB of 8% [2.4-2.6 ] GHz ,and The gain at less than 10 dB ARBW is 43 dB at 2.5 GHz, as shown in Figure 3. The best antenna performance was achieved with notch dimensions Wn, Ln as shown in Figure 2.

#### 4. Parametric Study

In this section, we examine the influence of the main parameters on the antenna performance. The outer width (W), the outer length (L), and the internal lengths (W2) of the square ring, which determine the circumference of the square ring are considered. While changing the parameter, the other parameters are fixed to their optimum values, as mentioned in the explanation of Figure 2. However, (W2) changes the variable around each square ring. For more clearly noticing the effect of (L) and (W), while the parameter (L) is adjusted and (W) varies.

Figure 4 and 5 shows the effect of W and L on antenna performance. Varying W and L that has a strong effect on the CP model, increasing W not only increases the circumference of the loaded square-ring but also increases the electrical path of the surface currents distributed on the parasitic loop, due to the electromagnetic coupling.

When the W was 31 mm, the reflection bandwidth ARBW of -10 dB at frequencies of 1.65 and 2.5 GHz was 60 and 200 MHz respectively, besides a higher gain. On the other hand, when W was 31.5 mm, we notice that the bandwidth still the same at the news frequencies of 1.63 and 2.52 GHz respectively. Also when W was 30 mm, the reflection bandwidth ARBW did not change at frequencies of 1.66 and 2.54 GHz respectively. For the Varying L, when the patch length was 28.5 mm, the reflection bandwidths ARBW of -10 dB were 80 and 220 MHz at frequencies of 1.5 and 2.5 GHz, respectively. When the patch length was 29 mm, we observed a new reflection bandwidth ARBW equal 60 and 200 MHz, for the same frequencies, besides a higher gain at 2.5 GHz. Either when L was 29.5 mm, a new reflection bandwidth ARBW of -10 dB was 50 and 180 MHz appears at the same frequencies, plus a higher gain at 1.5 GHz.

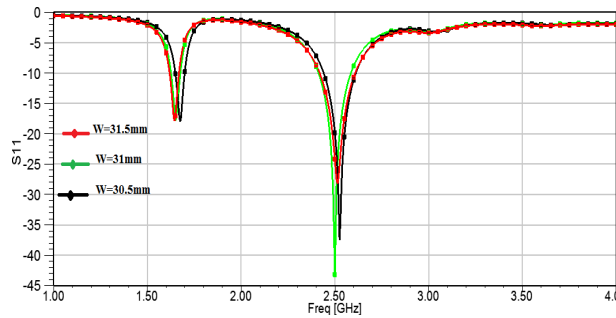


Figure 4 : S11: Effect of W on antenna performances

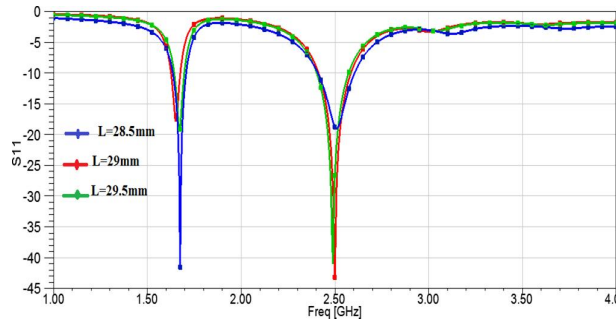


Figure 5 : S11: Effect of L on antenna performances.

Figure 6 shows the antenna performance in W2 variation. S11 from 3.4GHz CP mode is sensitive to W2 change, while medium and high frequency antenna performance is independent of W2 change. As the W2 increases, the circumference of the inner ring increases, and therefore, the CP mode moves at 3.4GHz to a lower frequency. This also confirms that setting the CP at 3.4GHz is excited by surface currents, near the inner edge of the load Square ring, in which the reflection bandwidth ARBW of -10 dB is 50 MHz [1.62-1.67 ] GHz and 200 MHz [2.4-2.6 ] GHz, for Varying W2 equal 4 mm. When W2 was 3.9 mm, the reflection bandwidth ARBW of -10 dB was 50 MHz [1.64-1.69] GHz and 210 MHz [2.41-2.62] GHz. When W2 was 4.1 mm, the reflection bandwidth ARBW of -10 dB was 50 MHz [1.65-1.7] GHz and 200 MHz [2.43-2.63] GHz.

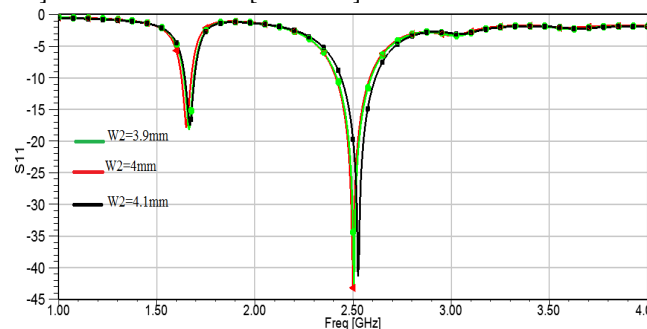


Figure 6 :S11: Effect of W2 on antenna performances.

The below table highlights different results of -10 dB reflection bandwidth ARBW and the return loss at specific frequencies for a several values of W, L and W2.

Table 1. : reflection bandwidth and Return loss for several values of W, L and W2.

Dimensions values (mm)	-10 dB Reflection Bandwidth (GHz)	Return loss (dB) at Frequency
W = 30.5	3% [1.61-1.66 ] GHz 8% [2.41-2.61 ] GHz	-18. 2 at 1.68 GHz -37.4 at 2.515 GHz
W = 31	3% [1.62-1.67] GHz 8% [2.4-2.6 ] GHz	-18. 2 at 1.665 GHz -43 at 2.5 GHz
W = 31.5	3% [1.63-1.68] GHz 8% [2.42-2.62 ] GHz	-18 at 1.645 GHz -28.2 at 2.525 GHz
L = 28.5	5.3%[1.63-1.72] GHz 8.7% [2.4-2.62 ] GHz	-42 at 1.68 GHz -18 at 2.5 GHz
L = 29	3% [1.62-1.67 ] GHz 8% [2.4-2.6 ] GHz	-18. 2 at 1.665 GHz -43 at 2.5 GHz
L = 29.5	3.5% [1.64-1.7] GHz 8% [2.4-2.6 ] GHz	-19. 2 at 1.638 GHz -41 at 1.5 GHz
W2 = 3.9	3% [1.64-1.69 ] GHz 8.3%[2.41-2.62]GHz	-18 at 1.65 GHz -42.8 at 2.504 GHz
W2 = 4	3%[1.62-1.67] GHz) 8%[2.4-2.6] GHz	-18. 2 at 1.665 GHz -43 at 2.5 GHz
W2 = 4.1	3% [1.65-1.7 ] GHz 8 % [2.43-2.63] GHz	-17. 6 at 1.7 GHz -42 at 2.52 GHz

### 5. PIN-Diode and Switching of the CP-Sense

The ability to switch between RHCP and LHCP in triple CP bands by using two PIN (D1, D2), Micro semi MPP4203 [26], which is used to direct and control the distribution of the surface current in the antenna and therefore, the currents flow tuning can be performed by varying state of the varactor diodes D1 and D2, Obtained using the reflection line calibration (TRL): resistor (RS = 3.5 Ω) and inductor (Ld = 0.45 nH) in series for the state of ON, capacitor (Ct = 0.08 pF) and resistor (Rp = 3 kΩ) in parallel and series with inductor (Ld = 0.45 nH) for the state of OFF. RHCP when D1 ON and D2 OFF, and LHCP radiates when D1 OFF and D2 ON.

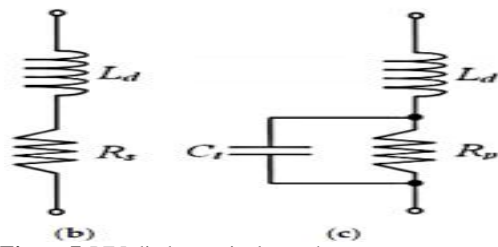


Figure 7 PIN diodes equivalent scheme

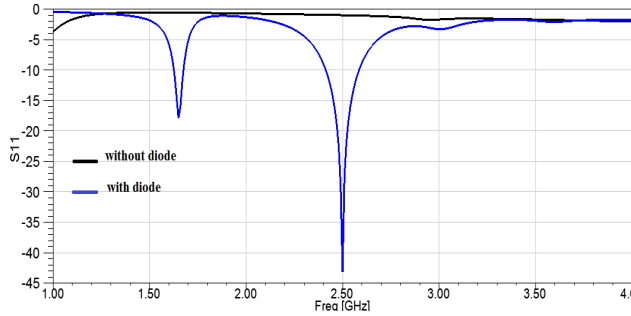


Figure 8 : Simulated reflection coefficients of the proposed antenna for both states With and Without diode.

In Figure 8, we see that for the case with the diode the reflection coefficient shows a good adaptation of the antenna around 2.5 GHz, which ARBW of reflection bandwidth of -10 dB is 8% [2.4-2.6] GHz, and the gain at less than 10 dB ARBW is 43 dB. On the other hand for the case without diode, the antenna does not make sense because reflection bandwidth ARBW of -10 dB is null.

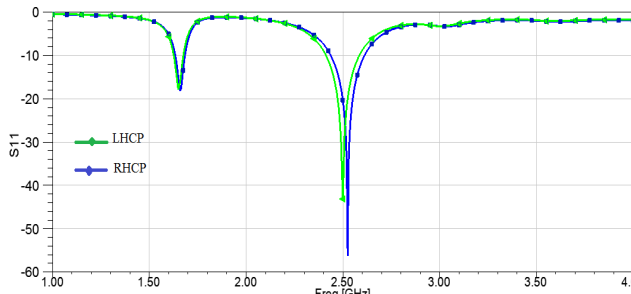


Figure 9 : Simulated reflection coefficients of the proposed antenna for both CP states.

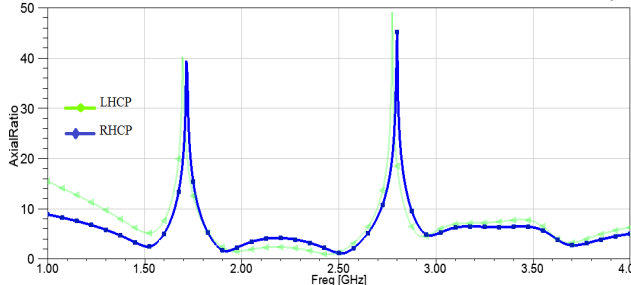


Figure 10 : Simulated ARs of the proposed antenna for both CP states.

In Figure 9 and Table II we see that the reflection coefficient for the polarization (LHCP) and the polarization (RHCP) show a good adaptation of the antenna around 2.5 GHz. The simulated 3 dB AR bandwidths are 52.8% [1.9-2.5] GHz for LHCP, 5.1% [1.9-2] GHz, and 8% [2.4-2.6] GHz for RHCP, at the UHF and 2.4 GHz bands as shown in Figure 10 and Table II.

Table 2. : Reflection bandwidth and AR bandwidths AND Return loss for both CP states.

CP states	3 dB AR bandwidths	-10 dB Reflection Bandwidth (GHz)	Return loss (dB) at Frequency
RHCP	5.1% [1.9-2] GHz 8% [2.4-2.6] GHz	3% [1.62-1.67] GHz 8% [2.4-2.6] GHz	-18. 2 at 1.65 GHz -43 at 2.5 GHz
LHCP	52.8% [1.9-2.5] GHz	3% [1.62-1.67] GHz 8% [2.44-2.64] GHz	-18. 4 at 1.6 GHz -56 at 2.5 GHz

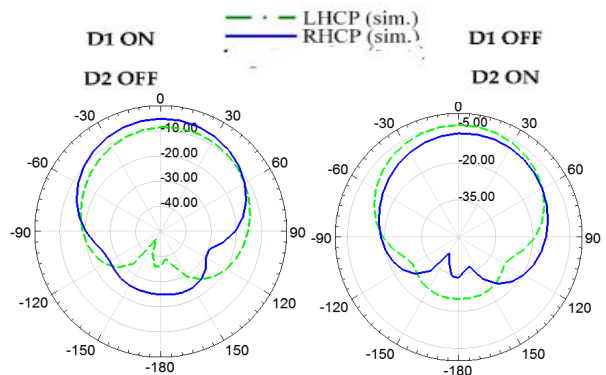


Figure 11 : Simulated radiation patterns on the x-z plane at 2.8 GHz.

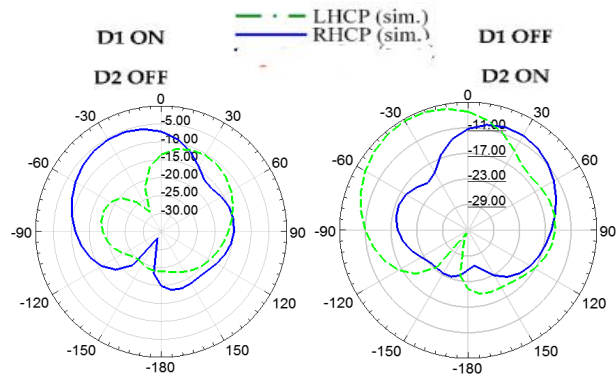
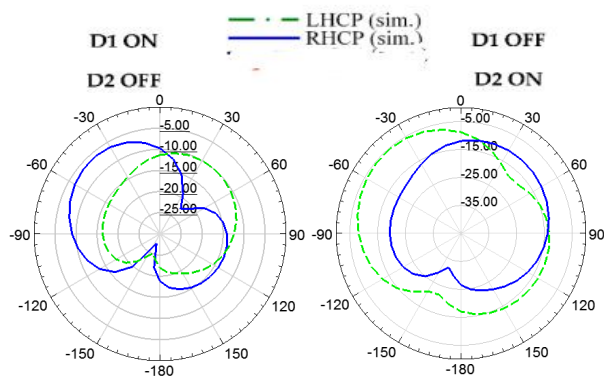


Figure 12 : Simulated radiation patterns on the x-z plane at 3.4 GHz.



**Figure 13** : Simulated radiation patterns on the x-z plane at 4 GHz.

The simulated normalized radiation patterns for 2.8 GHz, 3.4 GHz, and 4 GHz are displayed in Figures 11, 12 and 13. The proposed antenna radiates LHCP and RHCP. Besides, the radiation patterns of the proposed antenna at 2.8 GHz, 3.4 GHz, and 4 GHz, at all frequencies. The gain of LHCP was greater than RHCP when D1 ON and D2 OFF but on the contrary when D2 ON and D2 OFF.

#### 4. CONCLUSION

We have designed a patch antenna operating around 3 GHz. The antenna can operate around 3 GHz on left or right polarization according to the different states of the diode. The patch proposed a simple and easy to implement configuration is proposed for variable polarization antennas, validated by simulation results, the proposed antenna is suitable for wireless applications, as the operating range is modified by modifying the antenna design parameters such as W, L, and W2. This is the study obtaining reconfigurable CP radiation at three separate frequencies using only two diodes.

#### REFERENCES

[1] Josua, Setyo; Alvin, Gunawan; Muhammad, Rizki Sani; Gunawan, Wang . "Challenge of 5G Network Technology for Telemedicine and Telesurgery". International Journal of Advanced Trends in Computer Science and Engineering(ijatcse), Citation information: DOI 10.30534/ijatcse/2019/154862019

[2] D.,N,S, Ravi Kumar1 ; Dr,S,. Barani. " An Empirical Study on Issues Challenges Tools and Techniques of Vehicular Ad-Hoc Network Communications". International Journal of Advanced Trends in Computer Science and Engineering(ijatcse), Citation information: DOI 10.30534/ijatcse/2019/83842019

[3] Lin, W.; Chen, S.-L.; Ziolkowski, R.W.; Guo, Y.J. "Reconfigurable, wideband, low-profile, circularly polarized antenna and array enabled by an artificial

magnetic conductor ground". IEEE Trans. Antennas Propag. 2018, 50, 1564–1569

[4] Liu, Q.; Chen, Z.N.; Liu, Y.; Li, F.; Chen, Y.; Mo, Z. "Circular polarization and mode reconfigurable wideband orbital angular momentum patch array antenna". IEEE Trans. Antennas Propag. 2018, 66, 1796–1804.

[5] Tran, H.H.; Nguyen-Trong, N.; Nguyen, T.K.; Abbosh, A.M. "Bandwidth enhancement utilizing bias circuit as parasitic elements in a reconfigurable circularly polarized antenna". IEEE Antennas Wireless Propag. Lett. 2018, 17, 1533–1537.

[6] Wu, F.; Luk, K.M. "Wideband tri-polarization reconfigurable magneto-electric dipole antenna". IEEE Trans. Antennas Propag. 2017, 65, 1633–1641.

[7] Ge, L.; Yang, X.; Zhang, D.; Li, M.; Wong, H. "Polarization-reconfigurable magnetoelectric dipole antenna for 5G wi-fi". IEEE Antennas Wireless Propag. Lett. 2015, 14, 662–665.

[8] Hu, Z.; Wang, S.; Shen, Z.; Wen, W. "Broadband polarization-reconfigurable water spiral antenna for low profile". IEEE Antennas Wireless Propag. Lett. 2017, 16, 1377–1380.

[9] Kovitz, J.M.; Rajagopalan, H.; Rahmat-Samii, Y. "Design and implementation of broadband mems RHCP/LHCP reconfigurable arrays us"

[10] Li, L.; Zhang, X.; Yin, X.; Zhou, L. "A compact triple-band printed monopole antenna for WLAN/WiMAX applications". IEEE Antennas Wireless Propag. Lett. 2017, 16, 1504–1507.

[11] Huang, H.; Liu, Y.; Zhang, S.; Gong, S. "Multiband metamaterial-load monopole antenna for WLAN/WiMAX applications". IEEE Antennas Wireless Propag. Lett. 2015, 14, 662–665.

[12] Chen, H.; Yang, X.; Yin, Y.Z.; Fan, S.T.; Wu, J.J. "Triband planar monopole antenna with compact radiator for WLAN/WiMAX applications". IEEE Antennas Wireless Propag. Lett. 2013, 12, 1440–1443.

[13] L. Han, C. Wang, W. Zhang, R. Ma, and Q. Zeng, "Design of frequency- and pattern-reconfigurable wideband slot antenna", International Journal of Antennas and Propagation, vol. 2018, Article ID 3678018, 7 pages, 2018.

[14] L.-Y. Ji, P.-Y. Qin, Y. J. Guo, C. Ding, G. Fu, and S.-X. Gong, "A wideband polarization reconfigurable antenna with partially reflective surface", IEEE Transactions on Antennas and Propagation, vol. 64, no. 10, pp. 4534–4538, 2016.

[15] J.-F. Tsai and J.-S. Row, "Reconfigurable square-ring microstrip antenna", IEEE Transactions on Antennas and Propagation, vol. 61, no. 5, pp. 2857–2860, 2013.

[16] Liu, J.-C.; Zeng, B.-H.; Badjie,L.;Drammeh, S.; Bor, S.-S.; Hung, T.-F.; Chang, D.-C."Single-feed circularlypolarized aperture-coupled stack antenna with dual-mode square loop radiator". IEEE Antennas Wireless Propag. Lett. 2010, 9, 887–890.

- [17] Li, R.; Traille, A.; Laskar, J.; Tentzeris, M.M. **"Bandwidth and gain improvement of a circularly polarized dual-rhombic loop antenna"**. IEEE Antennas Wireless Propag. Lett. 2006, 5, 84–87.
- [18] Baik, J.-W.; Lee, T.-H.; Pyo, S.; Han, S.-M.; Jeong, J.; Kim, Y.-S. **"Broadband circularly polarized crossed dipole with parasitic loop resonators and its arrays"**. IEEE Trans. Antennas Propag. 2011, 59, 80–88.
- [19] Yang, Q.; Zhang, X.; Wang, N.; Bai, X.; Li, J.; Zhao, X. **"Cavity-backed circularly polarized soft-phased four-loop antenna for gain enhancement"**. IEEE Trans. Antennas Propag. 2011, 59, 685–688.
- [20] Chen, H.-D.; Tsai, C.-H.; Sim, C.-Y.-D.; Kuo, C.-Y. **"Circularly polarized loop tag antenna for long reading range RFID applications"**. IEEE Antennas Wireless Propag. Lett. 2013, 12, 1460–1463
- [21] Shi, S.; Ding, W.; Luo, K. **"Dual-band reconfigurable circularly polarized monopole antenna"**. Int J RF Micro C E. 2015, 25, 110–114.
- [22] Sharma, C.; Gupta, K.C. **"Analysis and optimized design of single feed circularly polarized microstrip antennas"**. IEEE Trans. Antennas Propag. 1983, 31, 949–955.
- [23] Lee, S.K.; Ooi, S.F.; Korolkiewicz, E.; Sambell, A. **"Explicit efficient coupling impedance formulas for the ringt-angled isosceles triangle and application to a circularly polarized truncated corners square patch antenna"**. IET Microw. Antennas Propag. 2007, 1, 1013–1019.
- [24] Chang, F.-S.; Wong, K.-L.; Chiou, T.-W. **"Low-cost broandband circularly polarized patch antenna"**. IEEE Trans. Antennas Propag. 2003, 51, 3006–3009.
- [25] Jung, J.; Choi, W.; Choi, J. **"A small wideband microstrip-fed monopole antenna"**. IEEE Antennas Wireless Propag. Lett. 2005, 15, 703–705.
- [26] Data Sheet of MPP4203 PIN Diodes, Microsemi, Application Note [Online]. Available online: <http://www.microsemi.com> (accessed on 21 February 2019).